

Hole lifetimes in [001] uniaxial stressed GaAs

S. Lee

Department of Physics, City College and The Graduate School of The City University of New York, New York, New York 10031

K. M. Yoo

Department of Electrical Engineering, City College and The Graduate School of The City University of New York, New York, New York 10031

R. R. Alfano

Departments of Physics and Electrical Engineering, City College and The Graduate School of The City University of New York, New York, New York 10031

H. Qiang and Fred H. Pollak

Department of Physics, Brooklyn College and The Graduate School of The City University of New York, Brooklyn, New York 11210

(Received 15 April 1992; revised manuscript received 14 October 1992)

The time-resolved photoluminescence (PL) spectra from *n*-type GaAs is nonexponential and is characterized by two decay constants (*A* and *B*). If the bimolecular recombination coefficient *B* is zero, the PL spectra have the familiar exponential time dependence (and are characterized by the recombination decay constant *A*). Application of uniaxial stress along [001] to the *n*-type GaAs sample causes the recombination decay constant *A* to increase, in agreement with the stress dependence of the matrix elements. The bimolecular recombination coefficient *B* is found to be stress independent. An increase in the density of the photogenerated holes *P*₀ as a function of stress is also observed. This is attributed to the stress dependence of the effective mass which changes the absorption coefficient. The stress dependence of the recombination decay constants *A* and *b* = *BP*₀ determines the stress dependence of the effective lifetimes of the light hole (parallel to the stress) in the *n*-type GaAs.

I. INTRODUCTION

Structural, electrical, and optical properties of semiconductors are dependent upon strain. Semiconductor properties which change under stress¹ are, for example, removal of degeneracies,²⁻⁴ shifts in the band edges,⁵⁻⁹ changes in the curvatures (effective masses)^{1,10-15} of the electronic band structure, changes in the interband matrix elements,^{1,16,17} and changes in the vibrational modes.^{18,19} These strain effects can influence carrier dynamics. The rate of photon emission is²⁰

$$\frac{4e^2}{3\hbar c^3} E_{c-v}^2 |\langle c | \hat{\mathbf{e}} \cdot \mathbf{p} | v \rangle|^2, \quad (1)$$

where E_{c-v} is the band-gap energy and $|\langle c | \hat{\mathbf{e}} \cdot \mathbf{p} | v \rangle|^2$ is the matrix element for the dipole transition from the conduction to the valence band. From the above equation, the radiative lifetime is stress dependent via the matrix element and E_{c-v} . There has been indirect evidence for the stress dependence of the hole lifetimes from line-shape analysis of resonance Raman scattering.^{21,22}

In this paper, we report on the photoluminescence (PL) from static uniaxial stressed *n*-type GaAs simultaneously resolved in both the frequency and time domains. The energy-resolved spectra give the shift in transitional energies as a function of stress. The change in the number of photogenerated carriers and the change in the hole lifetimes can be determined from the time-resolved spectra.

II. EXPERIMENTAL RESULTS AND DISCUSSIONS

A. Unstressed GaAs

In this experiment, 100-fs 620-nm pulses from the colliding-pulse mode-locked laser are used to probe the *n*-type GaAs sample. The PL from the sample is analyzed with a polarizer and is dispersed in energy and time by a spectrograph coupled with a synchroscan streak camera. A typical time-integrated spectra of the unstressed *n*-type GaAs at a sample temperature of 104 K is shown in Fig. 1. The PL peaks at 825 nm with a full width at half maximum (FWHM) of ~ 55 meV. This wide PL width is due to the 10^{18}-cm^{-3} doping. The time-resolved PL spectra of the unstressed *n*-type GaAs are shown in Fig. 2. There are several interesting features displayed in Fig. 2. First, the cooling of the hot electron-hole plasma (EHP) can be seen in the sharp peak in the 10-meV slices at 1580 meV of the unstressed GaAs PL spectra. Analysis of the first 100 ps for the 1580-meV band shows that the holes cool within the resolution of the experiment (12 ps). This is in agreement with previous results.²³

Another interesting feature displayed in Fig. 2 is the nonexponential decay of the PL. The PL is related to the recombination of the photogenerated electron-hole pairs [i.e., $n(t)$ electrons, $p(t)$ holes, with $n(t)=p(t)$]. From the detail balance requirement,²⁴ the relaxation of the carrier densities to the equilibrium carrier distribution (n_i ,

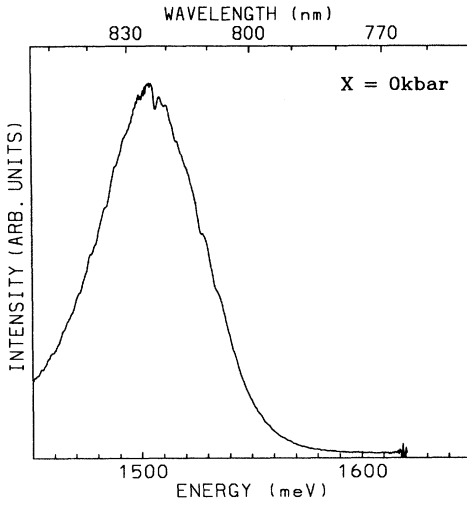


FIG. 1. A plot of the time-integrated spontaneous emission spectra from unstressed n -type GaAs at $T = 104$ K.

electrons and p_i holes) is given by

$$\frac{dn(t)}{dt} = \frac{dp(t)}{dt} \propto [n_i + n(t)][p_i + p(t)] - n_i p_i. \quad (2)$$

Ignoring reabsorption and including Auger-type transitions, the decay of the generated excess carriers can be described by²⁵

$$\frac{dp(t)}{dt} = -Ap(t) - Bp(t)^2 - Cp(t)^3, \quad (3)$$

where $A \equiv A_r + A_{nr}$, A_r is the radiative recombination coefficient, A_{nr} is the nonradiative recombination coefficient, B is the bimolecular recombination coefficient,^{24,26} and C is the recombination coefficient for collisional and phonon-assisted Auger transitions.²⁷ Since²⁷ $C \approx 10^{-29} \text{ cm}^6 \text{ s}^{-1}$ and the photogenerated EHP density is 10^{15} cm^{-3} , the third term on the right-hand side of Eq.

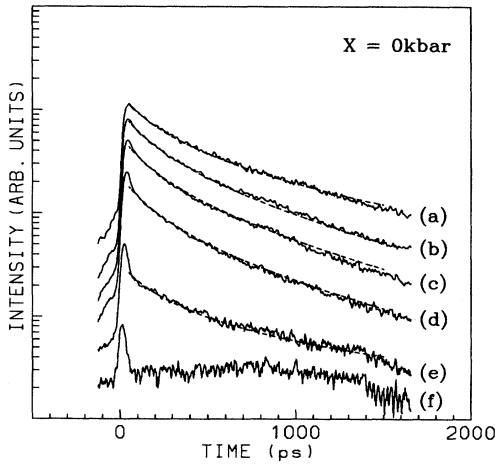


FIG. 2. Plots of the time-resolved spectra of unstressed n -type GaAs (—) for 10-meV slices at (a) 1480, (b) 1500, (c) 1520, (d) 1540, (e) 1560, and (f) 1580 meV. The dashed lines are the fit to the data using Eq. (4) (see text for details).

(3) is negligible compared to the two other terms.

With $C = 0$, the analytic solution to Eq. (3) is

$$\bar{p}(t) = [(1 + b_A)e^{At} - b_A]^{-1}, \quad (4)$$

where $b_A \equiv b/A$, $b \equiv BP_0$, and \bar{p} is defined by $p(t) \equiv P_0 \bar{p}(t)$. From a least-square fitting (see Fig. 2) to Eq. (4), it is found that $b = 4.6 \times 10^{-3} \text{ ps}^{-1}$ is approximately constant from 1470 to 1540 meV. The decay constant A is found to vary with energy (see Fig. 3). The decay constant A is seen to decrease for energies below 1500 meV, while above 1500 meV it is almost constant. The energy dependence of the recombination constant A in Fig. 3 has the following form:

$$A = A_1 + A_2 \left[\frac{h\nu}{\bar{E}} - 1 \right]^{1/2}. \quad (5)$$

A least-square fit yields values of $A_1 = 2.5 \times 10^{-4} \text{ ps}^{-1}$, $A_2 = 4.2 \times 10^{-3} \text{ ps}^{-1}$, and $\bar{E} = 1471 \text{ meV}$. It is interesting to note that the energy dependence of the recombination constant A is identical to the energy dependence of the allowed direct transitions.²⁸

The temperature-dependent direct intrinsic gap of GaAs is given by²⁹

$$\varepsilon_i(T) = 1519 \text{ meV} - \frac{(0.5408 \text{ meV K}^{-1})T^2}{T + 204 \text{ K}}, \quad (6)$$

and $\varepsilon_i(T = 104 \text{ K}) = 1500 \text{ meV}$. Of course, since the experimental sample is 10^{18} Si-doped n -type GaAs, the band gap is expected to be slightly smaller³⁰ than that given by Eq. (6). It can be seen that the fitted value for the effective band gap is quite reasonable.

B. Stressed GaAs (energy domain)

The apparatus used to apply stress to the GaAs sample has been described previously.¹⁶ Under uniaxial stress, the fourfold-degenerate valence band of GaAs is split into two spin-degenerate subbands (see Fig. 4). The shifts of

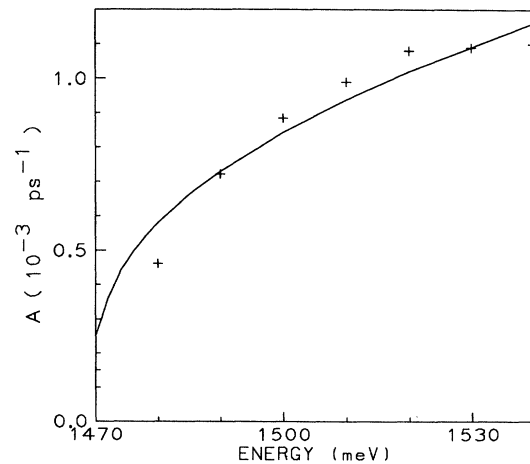


FIG. 3. A plot of the decay constant A (+) as a function of the transition energy. The solid line is the theoretical prediction from Eq. (6).

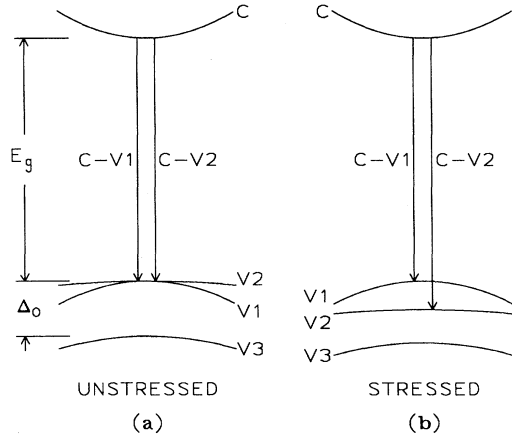


FIG. 4. The schematic diagram of the band structure of (a) unstrained and (b) strained GaAs. The conduction band is denoted by c , and the three valence subbands are labeled $v1$, $v2$, and $v3$.

the GaAs band edges under uniaxial stress have been well established by modulation spectroscopy. The shifts of the valence-band edges relative to the conduction-band edge are^{1,4}

$$\Delta E_{c-v1}(X) = \delta E_H - \frac{\delta E_{001}}{2} - \frac{\delta E_{001}^2}{2\Delta_0} + \dots, \quad (7a)$$

$$\Delta E_{c-v2}(X) = \delta E_H + \frac{\delta E_{001}}{2}, \quad (7b)$$

where⁵ $\delta E_H \equiv (3.85 \text{ meV/kbar})X$, $\delta E_{001} \equiv (6.13 \text{ meV/kbar})X$, and X is the compressive uniaxial stress.

The matrix elements for [001] uniaxially stressed GaAs have also been calculated.^{1,16} With stress, the matrix elements $|\langle c | \hat{\mathbf{e}} \cdot \mathbf{p} | v \rangle|^2$ for different polarization relative to the [001] stress axis (to first order in $\delta E_{001}/\Delta_0$) are proportional to

$$\begin{array}{c} \parallel \\ v_1 \\ v_2 \end{array} \begin{array}{c} 4 \left(1 + \frac{\delta E_{001}}{\Delta_0} \right) \\ 0 \end{array} \begin{array}{c} \perp \\ \left(1 - \frac{2\delta E_{001}}{\Delta_0} \right) \\ 3 \end{array} \quad (8)$$

This implies that the luminescence polarized parallel to the stress axis is composed of only $c-v1$ transitions. The luminescence polarized perpendicular to the stress axis comes from both the $c-v1$ and the $c-v2$ transitions. Therefore, a comparison of the parallel and perpendicular polarized PL will give information about the $c-v2$ transition.

The time-integrated spectra for PL polarized parallel and perpendicular to the [001] stress axis are plotted in Fig. 5. Also shown is the $c-v2$ transition which can be extracted, as noted above, by subtracting the parallel PL spectrum from the perpendicular PL spectrum. As a check, the sum of the parallel and perpendicular PL spectra agree quite well with the unpolarized spectra. The width of the $c-v2$ PL ($\sim 40 \text{ meV}$) is found to be slightly

narrower than the $c-v1$ PL (see Fig. 5). Both the $c-v1$ and the $c-v2$ PL are seen to blueshift according to Eq. (7).

C. Stressed GaAs (time domain)

Under uniaxial stress, the effective mass of holes in n -type GaAs changes. A stress-dependent effective mass leads to a stress-dependent absorption coefficient.³¹ The

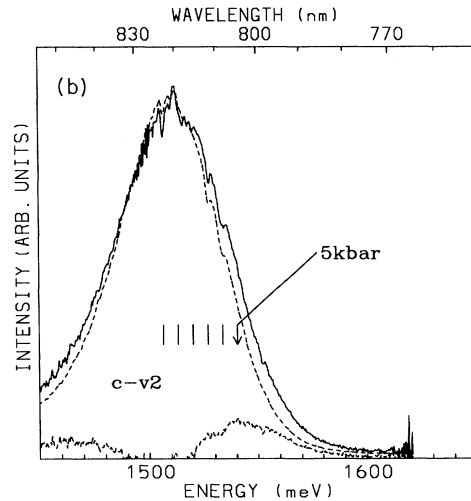
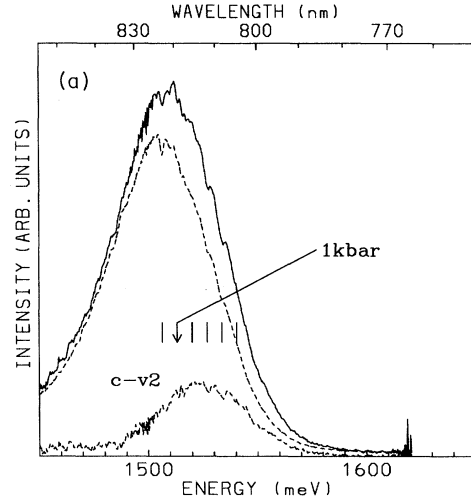


FIG. 5. (a) Plot of the time-integrated spontaneous emission spectra polarized \parallel (---) and \perp (—) to the [001] stress axis from n -type GaAs at $T=104 \text{ K}$ and $X=1 \text{ kbar}$. (b) Plot of the time-integrated spontaneous emission spectra polarized \parallel (---) and \perp (—) to the [001] stress axis from n -type GaAs at $T=104 \text{ K}$ and $X=5 \text{ kbar}$. The difference between the PL polarized parallel and perpendicular to the stress axis gives the contribution to the PL from the $c-v2$ transitions (see text). As a guide, the expected shifts of the $c-v2$ PL as a function of stress are plotted as tics.

stress-dependent absorption coefficient has been calculated¹⁰ using an effective mass that is linearly dependent on the stress (i.e., $m_\alpha^\beta = m_\alpha [1 + \delta_\alpha^\beta X]$ for $\alpha = v1$ or c and $\beta = \parallel$ or \perp), and is given by

$$\Delta\alpha(h\nu, X) = \left[\frac{\Delta_1(X)}{\Delta^0} \right]^{1/2} \left[\frac{\mu_\perp(X)}{\mu_0} \right]^{3/2} \times \frac{u}{2} \int_0^1 dz \frac{1 + (4u-1)z^2}{1 + (u-1)z^2}, \quad (9)$$

where $\Delta_1(X) \equiv \Delta^0 - \Delta E_{c-v1}(X)$, $\Delta^0 \equiv h\nu - E_g$, $\mu_0^{-1} \equiv m_c^{-1} + m_1^{-1}$, $u \equiv \mu_\parallel(X)/\mu_\perp(X)$, $\mu_\parallel(X)^{-1} \equiv m_{c\parallel}(X)^{-1} + m_{1\parallel}(X)^{-1}$, $\mu_\perp(X)^{-1} \equiv m_{c\perp}(X)^{-1} + m_{1\perp}(X)^{-1}$, m_c is the conduction-band effective mass, and m_1 is the $v1$ valence-band effective mass. For $\delta_\alpha^\parallel > 0$ and $\delta_\alpha^\perp < 0$, the absorption increases monotonically with stress. Using $\delta_c^\parallel = \delta_{v1}^\parallel = \delta_\parallel = 0.11 \text{ kbar}^{-1}$, $\delta_c^\perp = \delta_{v1}^\perp = \delta_\perp = -0.09 \text{ kbar}^{-1}$, and the GaAs effective masses³² ($m_c = 0.066$ and $m_1 = 0.082$) in Eq. (9), the change in the absorption coefficient is shown as a solid line in Fig. 6. An increase in the absorption coefficient implies an increase in the photogenerated carrier density (P_0). P_0 can be experimentally determined from the PL photon flux (F) at initial time²⁴ (i.e., $F \propto P_0^2$). Plotted as crosses in Fig. 6 are the changes in P_0 ($\Delta P_0 \equiv P_0[X]/P_0[X=0 \text{ kbar}]$) as a function of stress. There is good agreement between the experimental data and the theoretical prediction.

The time-resolved spectra of stressed n -type GaAs is qualitatively similar to the unstressed n -type GaAs PL. The change of the decay constants $\Delta b \equiv b(X)/b_0$ and $\Delta A \equiv A(X)/A_0$ as a function of stress is determined by least-square fitting to Eq. (4). ΔA is plotted in Fig. 7 together with the change in the matrix element as a function of stress [Eq. (8)]. It can be seen that the variation of A with stress can be attributed mostly to the stress dependence of the matrix elements. The decay constant b which is plotted in Fig. 6 also shows a strong stress

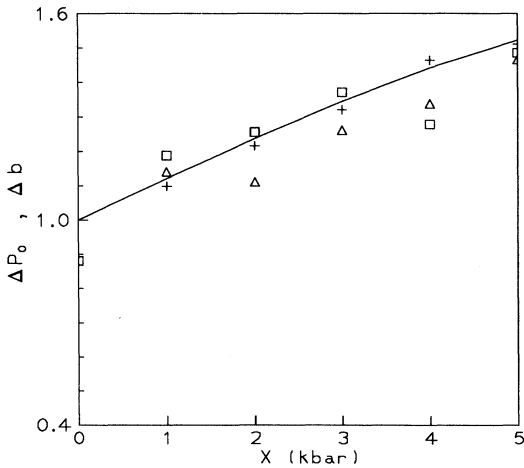


FIG. 6. A plot of the change in P_0 (+) together with the change in decay constant b (□ and Δ) as a function of stress. The solid line plotted is the theoretical prediction from Eq. (9) (see text).

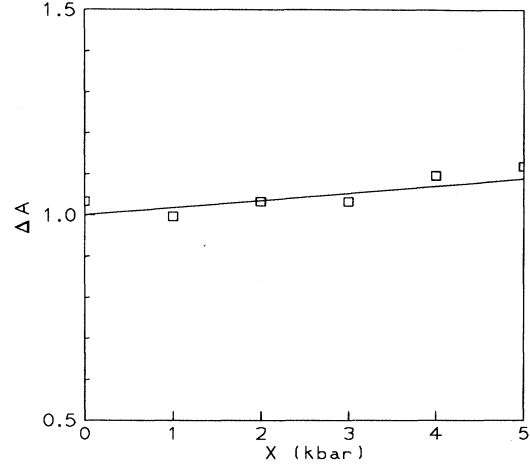


FIG. 7. A plot of the change in the decay constant A (□) as a function of stress. The solid line is the change in the matrix element as given by Eq. (8).

dependence. It appears that the stress dependence of b is the same as the stress dependence of P_0 . From this, one may conclude that the stress dependence of $b \equiv BP_0$ is due entirely to the stress dependence of P_0 and that the bimolecular recombination coefficient B is essentially independent of stress. From the experimentally determined value of the recombination constant b at $X=0 \text{ kbar}$ ($b_0 = 5 \times 10^{-3} \text{ ps}^{-1}$) and a photogenerated carrier density of 10^{15} cm^{-3} , the bimolecular recombination coefficient for this experiment is $B = b/P_0 = 5 \times 10^{-6} \text{ cm}^3 \text{ s}^{-1}$. This is different than the reported³³ values of $B = 5 \times 10^{-8} \text{ cm}^3 \text{ s}^{-1}$ to $B = 5 \times 10^{-10} \text{ cm}^3 \text{ s}^{-1}$. This difference can be attributed to surface recombination and a nonuniform photogenerated carrier density, which have a strong influence on the bimolecular recombination coefficient.³⁴

Since the decay of the PL is nonexponential, the lifetime of the hole is time dependent.²⁴ However, an effective lifetime can be defined as the time for the photogenerated carriers to decrease to e^{-1} of its initial value. The effective lifetime is²⁵

$$\tau_{\text{eff}} = \frac{1}{A_0 \Delta A} \ln \left[\frac{A_0 \Delta A e + b_0 \Delta b}{A_0 \Delta A + b_0 \Delta b} \right], \quad (10)$$

where $e = 2.71828$. Using the experimental values of $A_0 = 9 \times 10^{-4} \text{ ps}^{-1}$, $b_0 = 5 \times 10^{-3} \text{ ps}^{-1}$, and the ΔA and Δb shown in Figs. 7 and 6, respectively, the effective lifetimes of the $v1$ holes as a function of stress are plotted in Fig. 8. It can be seen that there is a 70-ps decrease of the $v1$ hole effective lifetimes as the stress on the n -type GaAs is increased from $X=0 \text{ kbar}$ to $X=5 \text{ kbar}$.

Turning our attention to the $c-v2$ transitions, from Fig. 5 it can be seen that the $c-v2$ PL is not clearly separated from the $c-v1$ PL and is also much weaker than the $c-v1$ transition. The $c-v2$ time-resolved PL can be obtained from the difference of the parallel and perpendicular PL (as described in Sec. II B). The stress dependence of the lifetimes of the $v2$ holes can be extracted from this approach. However, this means that the accuracy is not as

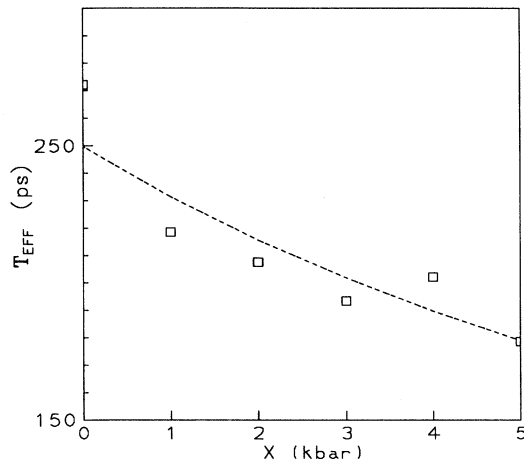


FIG. 8. A plot of the effective lifetimes of the v_1 holes (\square) as a function of stress. The dashed line is plotted as a guide.

good as for the $c-v_1$ transitions. Looking just at the time-resolved spectra of the $c-v_2$ transitions for $X=5$ kbar, the PL from the $c-v_2$ transitions has the same qualitative features as the PL from the $c-v_1$ transitions. Using Eq. (5), the bimolecular recombination coefficient ($B=5 \times 10^{-6} \text{ cm}^3 \text{ s}^{-1}$) for the $c-v_2$ PL is the same as for the $c-v_1$ transition at $X=5$ kbar. The $c-v_2$ decay con-

stant is $A \approx 8.4 \times 10^{-4} \text{ ps}^{-1}$ in contrast with the observed $A \approx 10 \times 10^{-4} \text{ ps}^{-1}$ for the $c-v_1$ transition at $X=5$ kbar. From Eq. (9), this yields only a difference of 8 ps between the effective lifetimes (τ_{eff}) of the $c-v_1$ and $c-v_2$ holes. Therefore, within the experimental accuracy, the decay times of the $c-v_2$ and $c-v_1$ transitions are almost the same. This is to be expected, since the holes are thermalized among the v_1 and v_2 valence bands within 11 ps.²³

In summary, three major strain effects have been observed in the hole dynamics of n -type GaAs. The transitional energies involving the v_1 and v_2 valence bands have been seen to blueshift. The stress dependence of the effective mass causes an enhancement of the absorption coefficient, which shows as an increase in the density of the photogenerated carriers as a function of stress. The time-resolved PL spectra from n -type GaAs is found to be nonexponential. The bimolecular recombination coefficient B is independent of stress, while the stress dependence of the decay constant A has the same stress dependence as the matrix elements. It is found that the effective lifetimes of the v_1 holes decrease as a function of stress.

ACKNOWLEDGMENTS

The City College is supported in part by organized research, Army Research Office, and Hamamatsu Photonics, and Brooklyn College acknowledges the support of a program of the New York State Science and Technology Foundation.

- ¹F. H. Pollak, in *Semiconductors and Semimetals*, edited by R. K. Willardson and A. C. Beer (Academic New York, 1990), Vol. 32, pp. 17–52.
- ²W. H. Kleiner and L. M. Roth, *Phys. Rev. Lett.* **2**, 334 (1959).
- ³F. H. Pollak, M. Cardona, and K. L. Shaklee, *Phys. Rev. Lett.* **16**, 942 (1971).
- ⁴M. Chandrasekhar and F. H. Pollak, *Phys. Rev. B* **15**, 2127 (1977).
- ⁵H. Qiang, F. H. Pollak, and G. Hickman, *Solid State Commun.* **76**, 1087 (1990).
- ⁶F. H. Pollak, *Surf. Sci.* **37**, 863 (1973).
- ⁷L. D. Laude, F. H. Pollak, and M. Cardona, *Phys. Rev. B* **3**, 2623 (1971).
- ⁸R. N. Bhargava and M. I. Nathan, *Phys. Rev.* **161**, 695 (1967).
- ⁹G. W. Arnold and D. K. Brice, *Phys. Rev.* **178**, 1399 (1969).
- ¹⁰N. K. Dutta, *J. Appl. Phys.* **55**, 285 (1984).
- ¹¹K. Suzuki and J. C. Hensel, *Phys. Rev. B* **9**, 4184 (1974).
- ¹²J. C. Hensel and K. Suzuki, *Phys. Rev. B* **9**, 4219 (1974).
- ¹³J. C. Hensel and G. Feher, *Phys. Rev.* **129**, 1041 (1963).
- ¹⁴H. Hasegawa, *Phys. Rev.* **129**, 1029 (1963).
- ¹⁵M. Cardona, *Phys. Rev.* **121**, 752 (1961).
- ¹⁶F. H. Pollak and M. Cardona, *Phys. Rev.* **172**, 816 (1968).
- ¹⁷C. S. Adams and D. T. Cassidy, *J. Appl. Phys.* **64**, 6631 (1988).
- ¹⁸E. Anastassakis, A. Pinczuk, E. Burstein, F. H. Pollak, and M. Cardona, *Solid State Commun.* **8**, 133 (1970).
- ¹⁹F. Cerdeira, C. J. Buchenauer, F. H. Pollak, and M. Cardona, *Phys. Rev. B* **5**, 580 (1972).

- ²⁰W. P. Dumke, *Phys. Rev.* **132**, 1998 (1963).
- ²¹C. Trallero-Giner, A. Alexandrou, and M. Cardona, *Phys. Rev. B* **38**, 10744 (1988).
- ²²A. Alexandrou, C. Trallero-Giner, G. Kanellis, and M. Cardona, *Phys. Rev. B* **40**, 1013 (1989).
- ²³K. Shum, Y. Takiguchi, J. M. Mohaidat, F. Liu, R. R. Alfano, and H. Morkoc, *Appl. Phys. Lett.* **56**, 2328 (1990).
- ²⁴H. B. Beeb and E. W. Williams, in *Semiconductors and Semimetals*, edited by R. K. Willardson and A. C. Beer (Academic, New York, 1972), Vol. 8, pp. 175–249.
- ²⁵H. J. Zarrabi, W. B. Wang, and R. R. Alfano, *Appl. Phys. Lett.* **46**, 513 (1985).
- ²⁶R. J. Nelson and R. G. Sobers, *J. Appl. Phys.* **49**, 6103 (1978).
- ²⁷M. Takeshima, *Phys. Rev. B* **23**, 6625 (1981).
- ²⁸J. I. Pankov, *Optical Processes in Semiconductors* (Dover, New York, 1975), p. 36.
- ²⁹J. S. Blakemore, *J. Appl. Phys.* **53**, R123 (1982).
- ³⁰Bo E. Sernelius, *Phys. Rev. B* **33**, 8582 (1986).
- ³¹N. K. Dutta and D. C. Craft, *J. Appl. Phys.* **56**, 65 (1984).
- ³²O. Madelung, in *Numerical Data and Functional Relationships in Science and Technology*, edited by K.-H. Hellwege, Landolt-Börnstein, New Series, Group III, Vol. 17a (Springer-Verlag, Berlin, 1985), p. 223.
- ³³M. Capizzi, S. Modesti, A. Frova, J. L. Staehli, M. Guzzi, and R. A. Logan, *Phys. Rev. B* **29**, (1984).
- ³⁴J. Shah, R. F. Leheny, and C. Lin, *Solid State Commun.* **18**, 1035 (1976).